Presented at the 18th IEEE Int. Conf. on Micro Electro Mechanical Systems (MEMS 2005), Miami Beach, FL, January, 2005.

MULTI-WATT ELECTRIC POWER FROM A MICROFABRICATED PERMANENT-MAGNET GENERATOR

S. Das[1], D. P. Arnold[2], I. Zana[2], J.-W. Park[2], J. H. Lang[1], and M. G. Allen[2]
[1]Massachusetts Institute of Technology, Cambridge, Massachusetts, USA
[2]Georgia Institute of Technology, Atlanta, Georgia, USA

ABSTRACT

This paper presents the design, fabrication, and characterization of permanent-magnet (PM) generators for use in microscale power generation systems. The generators are three-phase, axial-flux, synchronous machines, each consisting of a multi-pole surface-wound stator and PM rotor. The microfabricated windings, with small inter-conductor gaps and variable width geometry, are the key enabler for high power density. At a rotational speed of 120,000 rpm, one such generator demonstrates 2.6 W of mechanical-to-electrical power conversion and, coupled to a transformer and rectifier, delivers 1.1 W of DC electrical power to a resistive load. This Watt-scale electrical power generation demonstrates the viability of scaled PM machines for practical applications.

1. INTRODUCTION

Modern battery technologies have not kept pace with the rising demand for power by portable electronic devices. This has led to the need for alternative power sources such as MEMS-based electric generators that can produce 10–100 W of electrical power. Suitable electric generators could be powered by a variety of prime movers, including liquid flow, pressurized gas, or small combustion engines, such as a microscale gas turbine [1,2].

Previous work from this group focused on the use of magnetic induction machines [3,4] as potential electric generators. These machines were tested as tethered motors to verify their electromechanical performance and have demonstrated a peak torque of 2.5 μN-m [4] but were never tested in generating mode.

PM machines offer several advantages over induction machines, especially as the size is reduced [5]. First, the PM creates an independent source of rotor flux that is much larger than what can be produced by an induction machine of the same size, leading to much higher power densities. Second, since there are no eddy currents induced in the rotor, PM machine are more efficient.

Prior work has been done on planar MEMS PM machines. Low–speed, axial-flux PM motors have been demonstrated [6-8]. PM generators have also been investigated; one as a turbine generator for energy harvesting applications that produced 1.1 mW at 30,000 rpm [9] and another that has demonstrated high speed rotation (270,000 rpm) but has not yet generated power [10]. This paper focuses on the design, fabrication, and characterization of three-phase PM generators capable of spinning at high speeds (100,000+ rpm) and generating Watt-level power.

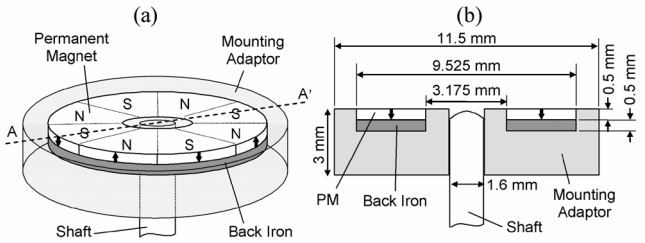

Figure 1. Multi-pole PM rotor and back iron mounted to shaft.

2. DESIGN

The generators are three-phase, eight-pole, axial-flux, synchronous machines [11], comprising a rotor with an annular PM and soft magnetic back iron and a stator with multi-turn surface windings on a soft magnetic substrate (back iron).

The rotor contains an eight-pole annular SmCo PM and a ferromagnetic FeCoV (Hiperco50) back iron (Fig. 1). The SmCo PM and FeCoV back iron are 500 μm thick, have an outer diameter of 9.525 mm, and inner diameter of 3.175 mm.

SmCo was selected for its combination of high energy product (BH_{max} ~ 240 kJ/m^3) for high energy conversion and high operating temperatures (T_{max} ~ 300°C). Although NdFeB has a higher energy product (BH_{max} ~ 400 kJ/m^3), it does not provide the necessary operating temperatures (T_{max} ~ 150°C) for integration with a combustion-driven microengine. However, it would be suitable for a low-temperature turbine generator. Hiperco50 was selected for the rotor back iron for its combination of high saturation flux density (B_s ~ 2.4 T) to prevent saturation and reasonably high permeability (μ_r > 3000).

Using this combination of high-performance magnetic materials (PM, rotor and stator back iron), the air gap can be made very large (300–500 μm). This allows the stator windings to occupy space in the air gap by placing them on the surface of a flat stator back iron rather than being embedded in slots and closed over with hats, as in the case of induction machines [3], greatly simplifying fabrication.

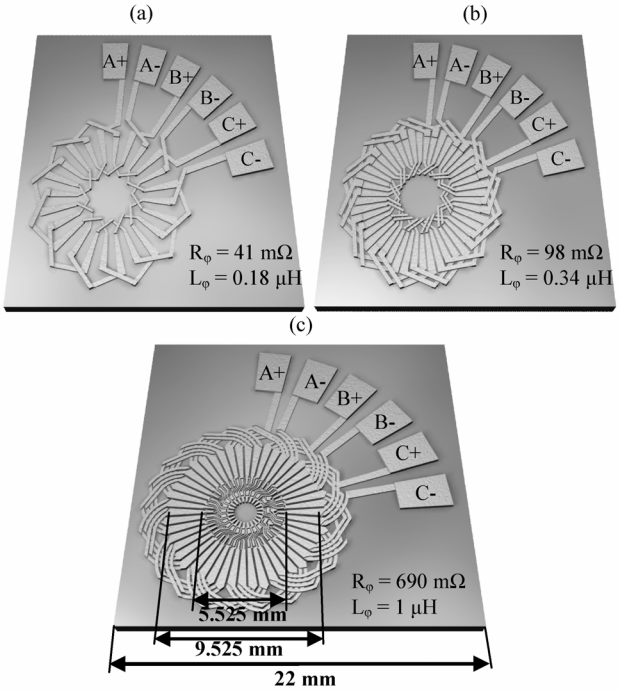

Figure 2. Conceptual drawings of (a) 1-turn/pole, (b) 2-turn/pole and (c) 4-turn/pole surface wound stators. The measured phase resistance and inductance is indicated for each type.

The surface wound stator has two other advantages over a conventional slotted stator. Since there are no slots, there is more surface area for the windings, which reduces conduction loss. Also, cogging, where the poles of the PM tend to align themselves with the gaps between the stator hats, producing torque pulsations and associated loss, is avoided.

The stator uses interleaved, three-phase, multi-turn electroplated Cu windings that are dielectrically isolated from a 1-mm thick NiFeMo (Moly Permalloy) substrate by a 3 μm spin-on-glass layer and/or 5 μm polyimide layer. NiFeMo is selected as the stator back iron (substrate) material for its combination of high permeability (μ_r > 1x10^4), low coercivity (H_c ~ 0.16 A/m) to minimize hysteresis losses, and commercial availability in sheets of suitable thickness.

Three different winding patterns are developed (1-, 2- and 4-turn/pole) to explore tradeoffs in output voltage/power and fabrication complexity (Fig. 2). The 1- and 2-turn/pole designs use simple single-layer windings with "crossovers" on the inner and outer end turns, while the 4-turn/pole design uses a full double-layer winding with more complicated end turns. In fact, the double-layer interleaved windings used in the 4-turn/pole machine match the complexity that is seen in macroscale machines [11].

For all three winding patterns, the radial conductors vary in width from 225 μm at the inner radius to 550 μm at the outer radius, with a 130 μm gap between adjacent radial conductors. The end turns of the 1-and 2-turn/pole machines have a minimum feature size of 100 μm and a minimum gap of 160 μm, while the end turns of the 4-turn/pole machine have a minimum feature size of 40 μm and a minimum gap of 40 μm. The coils are measured to be 80-120 μm thick.

3. FABRICATION

The stators are fabricated using electroplated windings (the most critical aspect) on 100-mm and 75-mm diameter magnetic substrates cut from 1-mm thick sheets of $Ni_{80}Fe_{15}Mo_5$ (Moly Permalloy). The complete winding fabrication process flow is shown in Fig. 3. First, to isolate the coils from the substrate, a dielectric layer is deposited (Fig. 3a). Initially, a spin-on-glass (SOG) process was used, where a 1 μm PECVD SiO_2 adhesion layer was deposited, followed by ~2 μm of Accuglass T-12 SOG, and finally, a 1 μm PECVD SiO_2 capping layer. It was later found that this layer sometimes suffered from cracking and/or pin-hole defects, resulting in shorts from the coils to the substrate, which reduced the yield. Therefore, this process is supplemented or replaced by the deposition of ~5 μm of PI-2611 polyimide.

The windings are constructed using a two-layer electroplating process [12,13] that is identical for the three different designs. First, a Ti/Cu seed layer is sputter deposited, and Futurrex NR9-8000P negative photoresist is used to pattern a mold for layer 1 (Fig. 3b). Cu is then electroplated up to the thickness of the mold (Fig. 3c). Next, the resist is stripped using Futurrex RR4 resist remover, and the seed layers are removed by wet etching (Fig. 3d). The via layer is then patterned using SU-8 2025 photosensitive epoxy, encapsulating layer 1 and opening vias for layer 2 (Fig. 3e). Then, a new Ti/Cu seed layer is sputter deposited, and layer 2 is patterned using NR9-8000P (Fig. 3f). Cu is again plated to form layer 2, with vias connecting to layer 1 (Fig. 3g). Finally, the Futurrex resist is stripped, and the seed layers are etched as before (Fig. 3h). The SU-8 is kept to provide additional mechanical support.

Fig. 4 shows examples of the three patterns of windings after fabrication. Note that with an increasing number of turns, the winding patterns, particularly the inner end turns, become quite complex, and hence more difficult to fabricate.

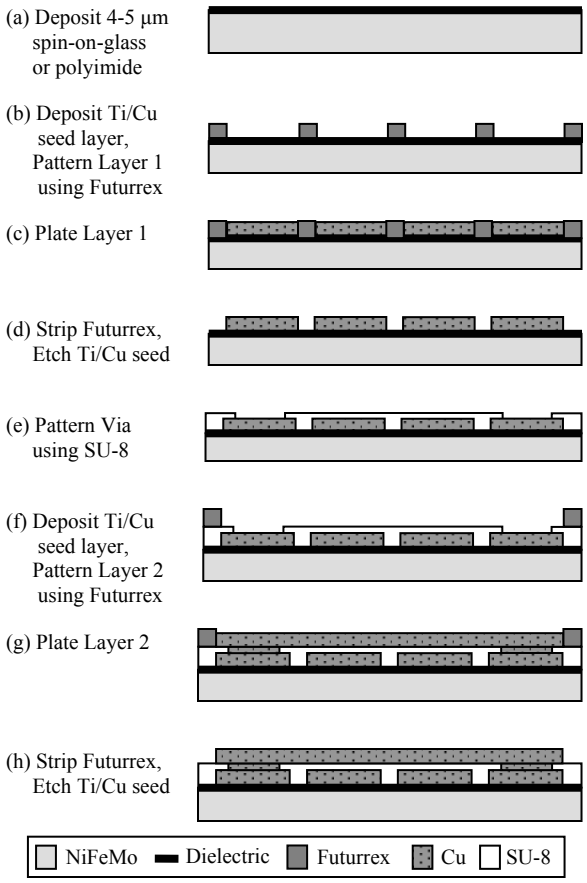

Figure 3. Stator winding fabrication process flow.

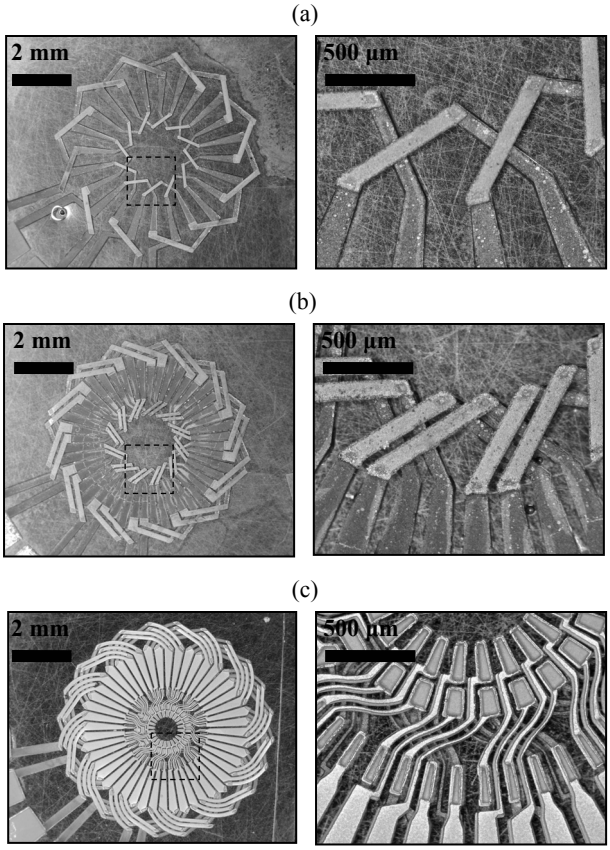

Figure 4. Fabricated stator windings: (a) 1-turn/pole, (b) 2-turn/pole and (c) 4-turn/pole machines.

The rotor components are conventionally machined, and the SmCo PM is magnetically patterned, as shown in Fig. 1a. Then, the PM and back iron are glued into the plastic (PMMA) adaptor, which is fit onto a 1.6 mm (1/16 in.) shaft for testing (Fig. 1).

For characterization, a test stand was developed to support spinning rotors in order to demonstrate electrical power generation while avoiding the design and fabrication complexities of integrated high-speed bearings. The test stand incorporates a high-speed, air-driven spindle to spin rotors with a controllable air gap over the surface of the stators, as depicted in Fig. 5. Powered by compressed nitrogen, the spindle rotates in excess of 350,000 rpm. The rotor/shaft assembly is mounted in the spindle, and the rotation speed is measured with an optical shaft encoder or, in the case of electrical machine tests, using the frequency of the generated output.

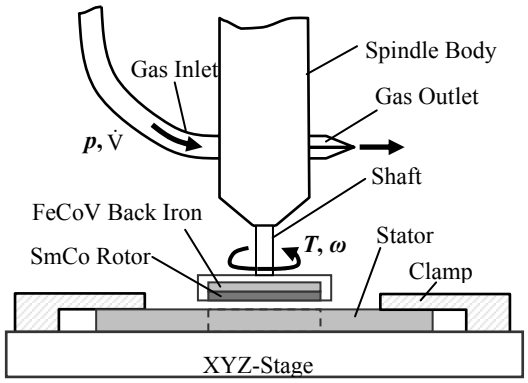

Figure 5 Spinning rotor test stand, depicting the air-powered spindle spinning a magnetic rotor over the surface of the stator.

4. RESULTS

The machines are first characterized in terms of their phase resistance, phase inductance and open-circuit voltage, V_{oc}. The machines are then connected to power electronics for power generation tests, which are conducted at varying load resistances and speeds with the rotor/stator air gap set to 100 μm.

The phase resistances for the 1-, 2- and 4-turn/pole machines are 41, 98 and 690 mΩ, while the inductances are 0.18, 0.34 and 1 μH, respectively. The resistance of the 2-turn/pole machine is about twice that of the 1-turn/pole machine, which is to be expected since a winding in a 2-turn/pole machine is twice as long as that in a 1-turn/pole machine yet has the same cross sectional area. The 4-turn/pole machine has a much higher resistance than the 2-turn/pole machine due to the fact that, in addition to having twice as many end turns, each end turn has a much smaller cross sectional area.

The open-circuit voltage, V_{oc}, of each machine is measured as a function of speed with the air gap set to 100 μm. A sample time waveform of V_{oc} for the 4-turn/pole machine is shown in Fig. 6 along with its power spectral density. Due to the large air gap, V_{oc} has low harmonic content. Similar waveforms were obtained for the 1- and 2-turn/pole machines. Fig. 7a shows V_{oc} varying linearly with speed and number of turns per pole. The open circuit voltage is also measured as a function of air gap. Fig. 7b shows the open circuit voltage for the same three machines at a rotor speed of 100,000 rpm. The open circuit voltage is a decreasing function of air gap due to the exponential decay of rotor flux in the air gap. Experimental measurements of V_{oc} versus speed, turns/pole and air gap agree well with analytical models of the machines [14].

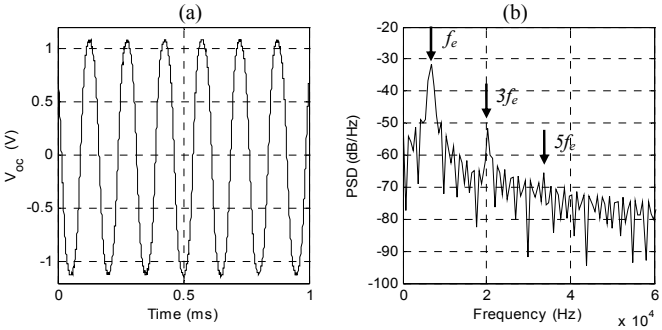

Figure 6. Open circuit voltage (a) time waveform and (b) power spectral density (PSD).

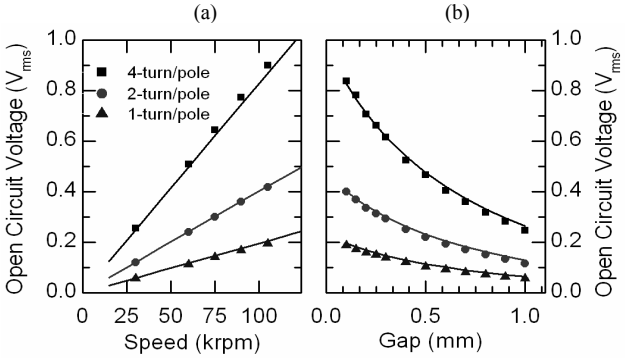

Figure 7. Open-circuit voltages (a) vs. rotational speed for 100 μm air gap and (b) vs. air gap at 100,000 rpm. Points represent measurements; curves represent analytical model.

To provide power to modern electronic devices that operate off a DC voltage, the AC generator voltages are first stepped up using a three-phase Δ/wye-connected transformer (1:6 turns ratio) and then converted to DC using a three-phase diode bridge rectifier. Schottky diodes are used because of their small forward voltage drops (0.3 – 0.4 V). The generator windings are connected in a wye configuration and tied to the Δ-connected primary side of the transformer, giving an overall step-up ratio of 18, to minimize the effects of the diode voltage drops. The generator and power electronics are modeled in PSpice [14] to predict power versus speed and load.

Fig. 8a plots the DC output power for the 2-turn/pole machine as a function of the speed for a fixed load of 30 Ω and confirms the expected quadratic dependence on speed up to 120,000 rpm. Fig. 8b shows the DC power delivered to the load as a function of load resistance (10–250 Ω) from the 2-turn/pole machine with the rotor spinning at 80,000, 100,000, and 120,000 rpm. At the three different rotation speeds, the generator delivered a maximum power of 0.46, 0.76 and 1.1 W, respectively. The machine shows the expected power transfer characteristics, with output power maximized under a matched load condition of $R_l \approx 25\ \Omega$. It should be noted that though the 4-turn/pole machine produces a higher voltage than the 2-turn/pole machine, it delivers less power due to its much larger phase resistance.

Efficiency is an important consideration in the generator design. Direct experimental measurement of the total generator efficiency, η_g, is not possible because the input mechanical power, P_m, was not directly measurable. Instead the total input mechanical power is estimated by summing the core loss and electrical power, $P_m = P_{core} + P_e$. The core loss, P_{core}, is extracted from the analytical machine model and consists of both eddy current and hysteresis losses. The electrical input power, P_e, is extracted from the PSpice models.

Fig. 9 shows the electrical efficiency, $\eta_e = P_o / P_e$, and total generator efficiency, $\eta_g = P_o / P_m$, for the 2-turn/pole machine as functions of load resistance and speed. The total generator efficiency is seen to be substantially lower than the electrical efficiency, suggesting the need for stator laminations to minimize eddy current loss. At the matched load condition of $R_l \approx 25\ \Omega$, the machine at 120,000 rpm shows an electrical efficiency of 43% and generator efficiency of 34%. Thus, it requires 3.2 W of mechanical power, of which 2.6 W is converted by the machine to electrical power, to deliver the 1.1 W output power. The electrical efficiency is dependent on speed due to non-linearities in the circuit, such as the nearly constant diode voltage drop and the non-linear transformer core loss as a function of voltage.

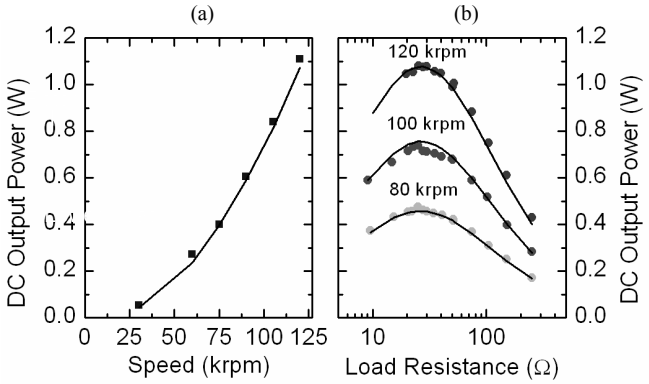

Figure 8. DC output power across the load resistor for 2-turn/pole machine at 100 μm air gap (a) vs. rotational speed for 30 Ω load and (b) vs. load resistance at 80, 100, and 120 krpm. Points represent measurements; curves represent PSpice model.

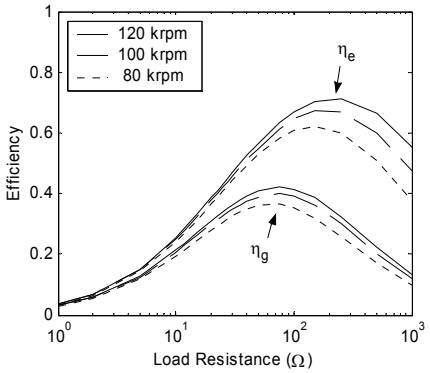

Figure 9. Electrical efficiency, $\eta_e = P_o / P_e$, and generator efficiency, $\eta_g = P_o / P_m$, for 2-turn/pole machine at 100 μm air gap.

5. CONCLUSIONS

Three-phase PM generators were designed and fabricated using a combination of microfabrication and precision machining/assembly. The machines were characterized using an air-driven spindle in generating mode. At 120,000 rpm, the 2-turn/pole machine demonstrated 2.6 W of mechanical-to-electrical power conversion and delivered 1.1 W of DC power to a resistive load. For an active machine volume of 110 mm^3 (9.5 mm OD, 5.5 mm ID, 2.3 mm thick), this corresponds to a power density of 10 MW/m^3. These results prove that Watt-level power production is achievable using miniaturized magnetic machines and demonstrate the viability of scaled PM generators for portable power applications.

6. ACKNOWLEDGEMENTS

This work was supported by the Army Research Laboratory (DAAD19-01-2-0010) under the Collaborative Technology Alliance in Power and Energy program, managed by Mr. John Hopkins (ARL) and Dr. Mukund Acharya (Honeywell).

7. REFERENCES

[1] S. A. Jacobson and A. H. Epstein, "An informal survey of power MEMS," ISMME 2003.

[2] A. H. Epstein, S. D. Senturia, et al., "Power MEMS and microengines," in *Digest Tech. Papers Transducers '97 Conference*, Chicago, June 16-19, 1997, pp. 753-756.

[3] H. Koser, F. Cros, M. G. Allen, and J. H. Lang, "A High Torque Density Magnetic Induction Machine," in *Digest Tech. Papers Transducers '01 Conference*, Munich, Germany, June 10-14, 2001, pp. 284-287.

[4] D. P. Arnold, et al., "Magnetic Induction Machines Embedded in Fusion-Bonded Silicon," in *Digest Tech. Papers Hilton Head '04 Conference*, Hilton Head Island, June 6-10, 2004, pp.129-132.

[5] O. Cugat, J. Delamare, and G. Reyne, "Magnetic Micro-Actuators and Systems (MAGMAS)," *J. Microelectromech. Syst.*, vol. 39, no. 5, pp. 3607-3612, Nov. 2003.

[6] B. Wagner, M. Kreutzer, and W. Benecke, "Permanent Magnet Micromotors on Silicon Substrates," *J. Microelectromech. Syst.*, vol. 2, no. 1, pp. 23-29, Mar. 1993.

[7] P.-A.Gilles, J. Delamare, O. Cugat, and J.-L. Schanen, "Design of a Permanent Magnet Planar Synchronous Micromotor," *Proc. 35th Mtg. IEEE Industry Appl. Soc.*, Oct. 2000, vol. 1, pp. 223-227.

[8] C. Yang, et al., "An Axial Flux Electromagnetic Micromotor," *J. Micromech. Microeng.*, vol. 11, pp. 113-117, 2001.

[9] A. S. Holmes, G. Hong, K. R. Pullen, and K. R. Buffard, "Axial-flow Microturbine with Electromagnetic Generator: Design, CFD Simulation, and Prototype Demonstration," in *Digest Tech. Papers MEMS '04 Conference*, Maastricht, Jan. 25-29, 2004, pp. 568-571.

[10] H. Raisigel et all, "Magnetic Planar Micro-Generator," *Proc. 18th Int. Workshop on High Performance Magnets and their Applications*, Annecy, France, Aug. 29-Sept. 2, 2004.

[11] A.E. Fitzgerald, C. Kingsley, Jr., S. D. Umans, *Electric Machinery*, 6th Ed., New York: McGraw Hill, 2002.

[12] J.-W. Park and Mark G. Allen, "Ultra Low-Profile Micromachined Power Inductors with Highly Laminated Ni/Fe Cores: Application to Low-Megahertz DC-DC Converters," *IEEE Trans. Magn.*, vol. 39, no. 5, pp. 3184-3186, Sept. 2003.

[13] M. G. Allen, "MEMS Technology for the Fabrication of RF Components," *IEEE Trans. Magn.*, vol. 39, no. 5, pp. 3073-3078, Sept. 2003.

[14] S. Das, "Magnetic Machines and Power Electronics for Power-MEMS Applications," *Ph.D. Thesis*, Massachusetts Institute of Technology, Cambridge, MA, To be submitted August 2005.